

¹ Consistency of geoid models, radar altimetry, and ² hydrodynamic modelling in the North Sea

J. Schall¹, A. Löcher¹, J. Kusche¹, R. Rietbroek¹, A. Sudau²

J. Schall, Bonn University, Nussallee 17, 53115 Bonn, Germany (jschall@uni-bonn.de)

¹Bonn University, Bonn, Germany,

²Federal Institute of Hydrography,

Koblenz, Germany.

3 **Abstract.** Radar altimetry, when corrected for tides, atmospheric forc-
4 ing of the sea surface, and the effects of density variations and mean and time-
5 variable currents, provides an along-track realization of the marine geoid. In
6 this study we investigate whether and how such an 'altimetric-hydrodynamic'
7 geoid over the North Sea can serve for validating satellite-gravimetric geoids.
8 Our results indicate that, using ERS-2 and ENVISAT along-track altime-
9 try and water levels from the high-resolution operational circulation model
10 BSHcmod, we do find distinct differences in RMS fits for various state-of-
11 the art satellite-only models (beyond degree 145 for GRACE-only, and be-
12 yond degree 185 for GOCE-models) and for combined geoid models, very sim-
13 ilar as seen in GPS-levelling validations over land areas.
14 We find that, at spectral resolution of up to about 200, an RMS fit as low
15 as about 7 cm can be obtained for the most recent GOCE-derived models
16 such as GOCO05S. This is slightly above what we expect from budgeting
17 individual errors. Key to the validation is a proper treatment of the spec-
18 tral mismatch between satellite-gravimetric and altimetric-hydrodynamic geoids.
19 Comparing data fits and error budget suggests that geoid truncation errors
20 residual to EGM2008 (i.e. EGM2008 commission and omission error) may
21 amount up to few cm.

1. Introduction

22 Radar altimeters measure the instantaneous distance from a satellite-borne nadir-
23 pointing antenna to the sea surface. Given a precise orbit and state-of-the-art media,
24 instrument and geophysical corrections, radar altimetry provides an along-track realiza-
25 tion of the instantaneous sea surface height (SSH) with respect to an ellipsoid.

26 When correcting such SSHs for water level variations associated with tides, atmospheric
27 forcing of the sea surface, salinity and density contrasts, and mean and time-variable
28 currents, one should arrive at a realization of the marine geoid. Traditionally, however,
29 corrected altimetric SSHs have been used more often to derive marine gravity anomalies,
30 and thus contribute to geoid determination indirectly at medium to short wavelengths.

31 Vice versa, satellite-gravimetric geoid modelling has been viewed as central in enabling
32 the full potential of radar altimetry for improving our knowledge of ocean processes. Ma-
33 jor recent improvements in spatial resolution and accuracy of the gravimetric geoid, in
34 particular following the data analysis of the GOCE mission, have lead to a wealth of
35 publication in this field (e.g. recent Special Issue in Newton's Bulletin, 2015). These ap-
36 proaches ultimately seek to improve ocean modelling through combining radar altimetry
37 and satellite gravimetry.

38 However, we feel it is reasonable to ask whether, for a well-monitored region like the North
39 Sea, altimetry combined with high-resolution operational hydrodynamic modelling can be
40 used to validate the satellite geoids, without relying on separate and possibly inconsistent
41 corrections for tides, inverse barometric effect, and dynamic topography.

42 Our approach is straightforward: We apply all standard corrections to along-track al-
43 timetry, except tide modelling and the correction for the inverse barometric effect. Subse-
44 quently, altimetric SSHs are further reduced to geoid heights by applying output from the
45 regional high-resolution 3D hydrodynamic model BSHcmod (Dick et al., 2001) forced by
46 atmospheric pressure and wind, astronomical constituents, and open-Atlantic boundary
47 conditions. These geoid heights are then temporally averaged and compared to satellite-
48 only and combined geoid models. Yet, an assumption we make is that the effect of
49 omission errors of the underlying geoid models can be mitigated in our assessment, in
50 that 'filling-up' with EGM2008 (i.e. adding signal from high-degree coefficients) allows
51 unbiased model comparisons at the same degree, and to some extent also across different
52 resolution.

53 Finally, we also investigate the ability of the hydrodynamic model to reproduce water
54 levels at a set of tide gauges. This, together with uncertainty estimates for altimetry and
55 geoid, is then combined into an error budget and compared to the fits obtained from the
56 data sets.

2. Data

2.1. Geoid Models

57 With the advent of the GRACE and GOCE satellite missions, a variety of geoid mod-
58 els have been determined and the need for validating (or at least comparing) them with
59 independent observations has become obvious.

60 In this study, we select a group of satellite-only and combined models as to cover the
61 progress in geoid modelling over the last years. A summary is provided in table 1. All

62 models are expressed in the zero tide reference system, and geoid heights are represented,
63 using Bruns' first approximation, above the GRS80 ellipsoid. We are aware that altimetry
64 data has been ingested in all combined models and that our consistency study should not
65 be misunderstood as a fully independent validation.

Tab. 1

66 Recent (i.e. release 5) GOCE-derived geoid models are thought to be accurate to about
67 1-3 cm at resolutions of degree 200 to 220 (from propagation of the GOCE variance covari-
68 ance matrix, Gruber et al., 2015), and GNSS-levelling comparisons (Voigt and Denker,
69 2015) appear to confirm these errors for some well-observed regions of the world.

2.2. Radar Altimetry Data

70 1 Hz radar altimetry data for the years 2000.0–2012.0 has been obtained for the ERS-
71 2 and ENVISAT satellites from the RADS data base (Naeije et al., 2008). ERS-2 and
72 ENVISAT have been flying in identical 35 day repeat orbits with an average track spacing
73 of less than 50 km in the North Sea.

74 We used cycles 0-169 of ERS-2 and 6-94 of ENVISAT data. Due to well-known problems
75 like scattering of the radar pulse close to the coastline, on tidal flats and in shallow
76 waters, and degraded quality of wet troposphere corrections, only data up to about 20 km
77 off the coastline is considered. All standard corrections from RADS have been applied
78 (ECMWF dry troposphere, MWR wet troposphere, solid Earth tide, GOT4.8 load tide, pole
79 tide, reference frame offset, ERS-2: DGM-E04 orbits, JPL GIM ionosphere, BM3 SSB,
80 ENVISAT: ESOC EIGEN-6C orbits, smoothed dual-frequency ionosphere, CLS SSB), but
81 excluding tides and inverse barometric (IB) effect.

82 Finally, sea surface heights have been transformed from the Topex/Poseidon ellipsoid to
83 the GRS80 ellipsoid. It is generally assumed that such (individual) sea surface heights
84 from ERS-2 and ENVISAT are precise at the 2-3 cm level excluding the coastal region.
85 Thus averaging of the order of $M = 100$ individual measurements (i.e. hydrodynamically
86 corrected altimeter measurements per reference track location) would bring errors down
87 to mm level, provided sea surface variability is taken care of.

2.3. Water levels

88 The mean dynamic topography in the North Sea reaches from about -40 cm off the
89 UK coast to 10 cm in the Skagerrak; the main reason for this being the large difference
90 in salinity between the North Sea and the Baltic, related to river inflow in the Baltic.
91 Changes in atmospheric conditions affect sea levels at the level of 0.3 m (through pressure
92 systems) and more (through wind), with surges reaching frequently up to 1 m and 2-3 m
93 in extreme cases. Large deviations from the theoretical inverse barometric effects exist
94 (e.g. Huess, 2001).

95 Tides in the North Sea represent a co-oscillating response to tides in the North Atlantic
96 (Banner et al., 1979). Tidal waves enter the North Sea through its Northern boundary
97 and through the strait of Dover. Subsequently, coastal geometry, bottom friction and
98 resonances play a role in generating North Sea tides. Seasonal variations of major con-
99 stituents such as M_2 are known to occur, and shallow-water constituents such as M_4 are
100 visible in altimetry (Andersen 1999). Moreover, a gradual increase in tidal range has been
101 observed at Dutch and German tide gauges in the Southern North Sea, starting around
102 1955 (Jensen and Mudersbach, 2006). The skills of conventional (deep-ocean) empirical

103 tide models used in altimetry are therefore limited in this region (Madsen et al., 2007).

104 Hydrodynamic models have found widespread application in the North Sea; for opera-
105 tional forecast but also for assessing effects of coastal engineering or sea level rise on
106 future tides. Along this line, BSHcmod (Dick et al., 2001) represents an operational baro-
107 clinic circulation and tide model for the North Sea, developed and run at the German
108 Federal Maritime and Hydrographic Service (BSH). BSHcmod is nested into a North At-
109 lantic model and driven by weather forecasts provided by the German Weather Service
110 DWD. The temporal resolution of the model is 15 min. For version 3, the spatial resolu-
111 tion has been $10' \times 6'$ over the North Sea and $1.6' \times 1'$ over the German Bight, whereas for
112 version 4 the resolution has been $5' \times 3'$ and $0.8' \times 0.5'$ accordingly. The model reproduces
113 14 partial tides. No radar altimetry data is assimilated in the model.

114 We used BSHcmod output for the same time frame as with altimetry, 2000.0–2012.0.
115 However, BSHcmod outputs originate from forecast model runs, and model updates take
116 place immediately with usually no overlapping time span that would allow data cross-
117 checking. In the investigated time frame, such a model update occurred on January 1,
118 2008, when BSHcmod switched from version 3 to version 4 at higher resolution. Unless it
119 is explicitly stated, all our comparisons refer to the composite model timeseries.

2.4. Tide Gauge Data

120 In order to allow for an independent assessment of the errors of modelled water levels,
121 we compare them to tide gauge observations (TGs). To this end, 15 TGs from the moni-
122 toring network of the German Federal Waterways and Shipping Administration (WSV),
123 all equipped with GNSS receivers, had been selected (we disregarded some gauges in

124 the Ems estuary after observing anomalous behaviour). The locations of the gauges are
 125 shown in figures 1-4 as red circles. All gauges except FINO1 (15.4.2008 – 21.6.2011) cover
 126 the whole time span of our investigation. TG values are recorded at 1min interval and
 127 downsampled to 15min, to be comparable with BSHcmod model output.

3. Methods

128 Our method is as follows: We compute altimetric-hydrodynamic geoid heights above
 129 the GRS80 ellipsoid along the satellite passes following Eq. (1),

$$N^{(a)} = h_{obs}(t) - \delta h(t) . \quad (1)$$

130 Here, $h_{obs}(t)$ is the altimetric SSH, and $\delta h(t)$ is the time-variable water elevation as
 131 computed by BSHcmod and spatially and temporally interpolated to the footprint loca-
 132 tion, thus including circulation, tides, wind stress and surges.

133 The $N^{(a)}$ relate to the altimeter footprints and thus, after this step, cover the North Sea
 134 with an along-track resolution of approximately 7 km, cross-track spacing of less than
 135 50 km, up to a distance of about 20 km to the coast.

136 In fact, each overpass of the altimeter provides an estimate $N_i^{(a)}$ for a given location.
 137 Thus, in order to suppress altimetric noise and unmodelled sea surface variability, we
 138 average these estimates into

$$\bar{N}^{(a)} = \frac{1}{M} \sum_i N_i^{(a)} \quad (2)$$

139 and derive the standard deviation $\sigma_{N_i^{(a)}}$ of the individual estimates:

$$\sigma_{N_i^{(a)}}^2 = \frac{1}{M} \sum_i (N_i^{(a)} - \overline{N}^{(a)})^2 . \quad (3)$$

140 As the ERS-2 and ENVISAT orbits vary by few km, evaluation of Eq. (2) requires that
 141 all altimetric heights within a certain region are binned onto a reference track position. To
 142 this end, all measurements within a cap of 5km size are assigned to a reference footprint
 143 and averaged in Eq. (2). Measurements exceeding five sigma are, finally, deemed as
 144 outliers and rejected in Eq. (2).

145 We then compute the corresponding gravimetric geoid heights above the GRS80 ellipsoid,
 146 at the reference footprint locations, following Eq. (4),

$$N^{(g)} = N_{j;n}^{(g)} + \delta N^{(g)} . \quad (4)$$

147 In the above, $N_{j;n}^{(g)}$ is the geoid height obtained from the satellite-gravimetric model
 148 MODEL_j, complete up to spherical harmonic degree n (which may be lower than the model's
 149 maximum degree).

150 In order to mitigate the spectral inconsistency between $N_{j;n}^{(g)}$ and $N^{(a)}$, we add a high-
 151 resolution ('fill-up') geoid contribution $\delta N^{(g)}$ from EGM2008 (complete from degree n up
 152 to full model resolution, i.e. 2190). This is of course the same as if we would smooth the
 153 $N^{(a)}$ by removing the high-frequency geoid contribution. An alternative way would be
 154 applying spectral or spatial filtering to the $N^{(a)}$ directly; however, this poses problems in
 155 coastal regions and due to the limited size of the North Sea we refrain from this option.

156 However, our approach for mitigating spectral inconsistency is consistent with what is

157 applied currently in land-based GNSS-levelling validations of the recent GOCE models
 158 (e.g. Voigt and Denker, 2015, for Germany, and Šprlak et al., 2015, for Norway).

159 Our metric of comparison is the spatial RMS of differences, from P altimeter footprints

$$RMS^2 = \frac{1}{P} \sum_{p=1}^P \left(\overline{N}^{(a)} - N^{(g)} - c \right)^2 \quad (5)$$

160 with c being the (weighted) spatial average of the $\overline{N}^{(a)} - N^{(g)}$,

$$c = \sum_{p=1}^P \omega_p \left(\overline{N}^{(a)} - N^{(g)} \right) \quad (6)$$

161 and ω_p following from the sigmas per location

$$\omega_p = \frac{\frac{1}{\sigma_{N_p^{(a)}}^2}}{\sum_{i=1}^P \frac{1}{\sigma_{N_i^{(a)}}^2}} . \quad (7)$$

162 The RMS, Eq. (5), could be compared to error propagation applied to Eqs. (2) and
 163 (4). Assuming we know the a priori errors of altimetric measurement $\sigma_{h_{obs}}$, water level
 164 modelling $\sigma_{\delta h}$, commission error $\sigma_{N^{(g)}}$ and omission error $\sigma_{\delta N^{(g)}}$ of the geoid model (or, in
 165 case of 'fill-up', of EGM2008), the predicted fit will be of the order of

$$\sigma_{\overline{N}^{(a)} - N^{(g)}}^2 = \frac{1}{M} \sigma_{h_{obs}}^2 + \frac{1}{M} \sigma_{\delta h}^2 + \sigma_{N^{(g)}}^2 + \sigma_{\delta N^{(g)}}^2 . \quad (8)$$

166 With what has been said before ($\sigma_{h_{obs}}$ 2-3 cm, $\sigma_{N^{(g)}}$ 2-3 cm), assuming $\sigma_{\delta h}$ to 20-30 cm,
167 see section 4.2, and averaging of the order of $M = 100$ individual measurements, we
168 would expect to see a noise floor of 4-5 cm in the RMS difference between altimetric-
169 hydrodynamic and gravimetric geoid heights. $\sigma_{\delta N^{(g)}}$ is particularly difficult to estimate,
170 and we postpone a discussion to a later section. Higher RMS at a given location indepen-
171 dent of the used geoid model may point at hydrodynamic modelling problems, while we
172 would expect to see geoid model performance in varying RMS as per location, for different
173 truncation and fill-up degrees.

174 We notice that in the above error budget, as well as for all metrics provided in the
175 subsequent results section, errors are assumed as uncorrelated. In reality, altimetry mea-
176 surements are known to be correlated along-track due to orbit errors, and geographically
177 due to errors in media and sea state corrections. Hydrodynamically modelled water levels
178 tend to be affected by systematic phase errors, which map into temporal correlation and
179 large RMS values in error time series. Geoid model errors, finally, are inevitably spatially
180 correlated due to the way they are computed. With these caveats in mind, our errors
181 and RMS fits should be seen as worst case assumptions; yet since RMS fits provide the
182 standard methodology in model evaluations we think for the sake of repeatability and
183 comparability our approach is the most reasonable at the time of being.

4. Results

4.1. Altimetric-Hydrodynamic Geoid

184 Figs. 1 and 2 display maps of the temporal mean $N^{(a)}$ from BSHcmod version 3 (2000.0-
185 2008.0) and version 4 (2008.0-2012.0).

186

Fig. 1

187

Fig. 2

188

189

190

191

192

193

194

195

196

197

198

199

200

201

202

203

204

205

206

207

It is obvious that a dm-size offset in mean sea surface between the two model versions exist over the North Sea, while this appears not the case for the Skagerrak and large parts of the Baltic Sea (not shown in the figure). This was noticed already in Weiss (2013) for a limited number of T/P and Jason crossover points, and we discuss it below. Apart from this, the mean modelled water level appears similar to earlier altimetric studies (Madsen et al., 2007). The mean water level or dynamic topography in BSHcmod is characterized by a general East-West sloping with gradients not exceeding 17 " (except coastal areas). For reference, the full RMS water level variability of BSHcmod version 3 is shown in Fig. 3, with an average RMS of 44 cm (for version 4, this is very similar with a slightly higher average RMS of 47 cm, not shown here).

Fig. 3

Next, in Fig. 4 a spatial representation of the empirical $\sigma_{N_i^{(a)}}$ is provided; this map tells where hydrodynamically corrected water levels from individual altimetry tracks fit less well (off the UK coast and in the strait of Dover, and thus where weights ω_p will be low), and where they fit very well (Norwegian coast, Skagerrak). Larger $\sigma_{N_i^{(a)}}$ are clearly associated with regions of higher variability of water levels due to tides and surges; our comparison may thus aid, outside of the scope of the present study, in guiding efforts directed at model improvements.

One may ask, whether and to what extent the mean water level offset between model version time series represents an artefact – and may adversely affect our comparisons – and to what extent it reflects a change in real conditions. In fact we have reasons to assume that changes in the model resolution, model forcing and data assimilation system,

Fig. 4

208 and possibly in vertical referencing, are responsible for this effect. But since neither
209 an extended overlap period for both model versions is provided, nor does a consistent
210 reanalysis exist, we can only speculate about this. A comparison of Fig. 3 and 4 reveals
211 that differences are generally below 8-10 cm in the North Sea interior, and larger along the
212 UK shelf and the Channel where water level amplitudes are largest. Yet, we find that the
213 spatial average of the $\sigma_{N_i^{(a)}}$ amounts to 15.0 cm; whereas when we evaluate only over the
214 BSHcmod version 3 time span we arrive at little improvement with 14.8 cm, and 13.3 cm
215 for model version 4. Future work would therefore likely benefit from concentrating on the
216 version 4 time series alone, but at the time being, with only few years, we rather use the
217 full time series for the generation of the $\overline{N}^{(a)}$.

4.2. Comparison at tide gauges

218 Modelled water levels are projected to TG locations and compared to 15min obser-
219 vations, after removing a local temporal mean. Again, we evaluate separately the two
220 BSHcmod model time series: version 3 (2000.0-2008.0) and version 4 (2008.0-2010.0).

221 Table 2 shows the RMS difference between modelled and observed water levels, and Fig.
222 5 provides exemplary time series (Borkum-Fischerbalje, TGBF). We note that the model
223 captures tidal and wind-driven water level ranges typically at the 5-20 cm level, but that
224 it sometimes (here days 23-27) lags behind and this may dominate the tabulated RMS. Tab. 2

225 While individual (relative) TG readings are generally assumed to be accurate at the few
226 cm level, we find RMS differences at the dm level, with the largest differences in the Ems
227 and Weser estuaries. This suggests that the model has its largest difficulties in shallow
228 regions, as may be expected. Furthermore, we find that application of model version

229 4 generally reduced the RMS, with greatest improvements for those stations that have
230 exceptional high differences in version 3 (e.g. Bremerhaven TGBH, Knock TGKN, and
231 Wilhelmshaven TGWH). With what has been said before, switching from model version
232 3 to 4 appears to have bigger effects on TG RMS reduction compared to altimetry.

Fig. 5

233 This comparison suggests that modelled water levels, off the estuaries, can be assumed
234 as having errors at the 20-30 cm level. This, however, applies to individual readings.
235 Assuming errors as uncorrelated, and averaging of the order of 100 water levels, should
236 reduce the error level down to 2-3 cm (except estuaries).

4.3. Satellite-Gravimetric Geoids

237 Fig. 6 displays the RMS fit of the global geoid models (see table 1), truncated at various
238 degrees, when compared track-wise with the altimetric-hydrodynamic geoid heights. As
239 discussed before, the gravimetric geoid error consists of the model or commission error
240 and the omission error, due to missing real short-wavelength geoid signal. The figure
241 can be interpreted as follows: As long as the error of an added coefficient of subsequent
242 degree does not exceed the signal, increasing the degree of truncation will reduce the total
243 error; thus resulting in a decreasing trend in the RMS error curve. When the error curve
244 remains at the same level or rises, the error is likely at least as large as the signal, which
245 means that the specific model has reached its maximum resolution.

Fig. 6

246 As we will use the EGM2008 model, subsequently, to mitigate the spectral mismatch be-
247 tween altimetric-hydrodynamic geoid heights and those from gravimetric models, it is
248 appropriate to discuss the fit of the full EGM2008 model to altimetry first, for $N^{(g)} =$
249 $N_{EGM2008;2190}$. We find the RMS steeply decreasing from $> 40\text{cm}$ at degree 100, entirely

250 dominated by truncation errors, levelling off to about 15cm at degrees 240 to 260 (for
251 comparison, with the global ocean tide model GOT4.8, (Ray, 1999, updated), standard
252 IB corrections, but no MDT model removed, at degrees 240 to 260 this would be about
253 22cm). At full model resolution (degree 2190), the RMS of EGM2008 amounts to 6.4cm.

254 We find that the GRACE-only models ITG-Grace2010S and ITSG-Grace2014S can re-
255 solve gravity signal up to d/o 160 and 170, respectively. One should note that hardly
256 any difference between the two models would be visible in a global degree variances plot.
257 Improvements through adding more data become obvious when looking at the GOCE
258 models. We find that early GOCE models such as ITG-Goce02 contain signal up to d/o
259 205, while the latest models, which are based on the entire mission data, contribute to
260 the North Sea geoid even up to d/o 245.

Fig. 7

261 In Fig. 7, the same global geoid models are shown in comparison to the altimetric-
262 hydrodynamic heights, but this time after reducing the omission error through fill-in with
263 EGM2008. At lower degrees, the commission error, which is expected to grow with the
264 degree of truncation, appears small and the misfit is likely dominated by errors in altime-
265 try and/or hydrodynamic modeling. The various data sets agree at a level of 7cm (for
266 GOT4.8 as above, this would be about 17cm), provided that the geoid is represented at
267 moderate spatial resolution. Divergence of the error curves indicate at which degree a
268 specific geoid model deteriorates in accuracy.

269 As expected, the errors (or rather misfits) of the latest GRACE-only solution ITSG-
270 Grace2014S diverge at higher degree (d/o 150) compared to the earlier ITG-Grace2010S
271 (d/o 145). For the GOCE models of the second and last generation, errors grow ex-

272 ponentially from 185 and 225, respectively. The error curves of the latest GOCE and
273 GRACE/GOCE combination models are very similar, which indicates that the contribu-
274 tion of the combined data is mainly in the lower degrees.

275 The new GFZ solution EIGEN-6C4 has been chosen as an additional combination model
276 besides EGM2008 as it includes GOCE data. The model performs quite well and it
277 achieves RMS values nearly as low as the EGM2008 'noise floor' 6.4cm of while its curve
278 never falls below that of EGM2008.

Tab. 3

279 As expected, the regional models that are based on recent satellite-gravimetric models
280 perform very well, for they have been adapted to the study area. For the gridded models
281 the comparison was applied at full resolution only and the resulting RMS, min and max
282 values are summarized in table 3. GCG2011 was warped to coincide with the geoid heights
283 calculated at GPS/levelling points, but over the North Sea no corrector surface has been
284 applied and the agreement is excellent. However, the model is defined in the area of the
285 exclusive economic zone of Germany, which only covers a small part of the North Sea.
286 It is thus questionable whether this result is comparable to the other models. EGG08
287 also achieves a good result, which is nearly as low as that of EGM2008. The RMS fit of
288 NLGEO2013 is slightly higher, likely since the density of surface data used for this model
289 is higher over the dutch mainland and waters compared to e.g. German and UK coast
290 and waters (Slobbe, personal communication).

291 At the first glance EGM2008 seems to be superior to all the other models. However, one
292 has to remember that EGM2008 already includes altimetry data and a good consistency
293 is thus not surprising. Incidentally, the same is true for all combined models. Moreover,

294 degree-wise 'augmentation' of harmonic coefficients is not optimal in a statistical sense.
295 The coefficients, in particular those of the GOCE models, are highly correlated and provide
296 a good solution only when used in linear combination. When this basic principle is ignored,
297 the result can hardly be predicted.

298 Finally, we notice that estimating c in Eq. (5) led to an offset of about 17.3 cm, very
299 consistent across all tested geoid models and nearly independent of the model expansion
300 degree. A possible explanation for this could be that application of the hydrodynamic
301 model realizes the reduction of water heights to an equipotential surface different from
302 the geoid. BSHcmod has not been constrained by altimetry but likely by tide gauges
303 in procedures not well known to us; so we hypothesize that unspecified vertical model
304 referencing in combination with other possible reference system issues is responsible for
305 the offset. Due to the difference between hydrodynamic model versions we used, our
306 estimate for c depends on the time frame (19 cm with version 3 and 13 cm with version
307 4).

5. Conclusions

308 From budgeting the various error sources, we expect to see a noise floor of about 4-5 cm
309 in the RMS difference between altimetric-hydrodynamic and (state-of-the art GOCE-
310 derived) gravimetric geoid heights.

311 We find distinct differences in RMS fits for satellite-only models, combined geoid models,
312 and regional geoid models. As maybe expected, GRACE-based models resolve up to d/o
313 170, early GOCE models up to about d/o 205, while latest models contribute to the North

314 Sea geoid up to d/o 245. When correcting for omission errors, the models agree with hy-
315 drodynamically corrected altimetry at the 7 cm level, provided the geoid is represented
316 at moderate spectral resolution (up to d/o 230 for most recent GOCE models). This is
317 slightly above what we expect from budgeting individual errors, and the reason may be
318 related to a missing estimate of the geoid omission error (with respect to EGM2008). For
319 higher truncation degrees, distinct differences between earlier and more mature models
320 evolve. As expected, GRACE-only derived models perform less well beyond about de-
321 gree 140 compared to recent GOCE models. We find best RMS fits for recent combined
322 regional models, even down to 3-4 cm (but in a limited area); yet such models are not
323 completely independent of altimetry. A caveat is that EGM2008 has been used as a fill-in
324 in all our computations, in line with what is applied in terrestrial GNSS/levelling valida-
325 tion studies.

326 Such land-based tests (Voigt and Denker, Gruber 2015) provide fits down to few cm and
327 may be likely more accurate compared to our validation, but strong differences between
328 regions exist, depending on quality of GNSS data and levelling, but in particular also on
329 the areal extension.

330 Finally, we have found an offset of about 17cm between gravimetric and altimetric-
331 hydrodynamic geoids, consistent across all tested models. We hypothesize that the reason
332 for this may be related to the vertical referencing of the hydrodynamic model.

333 In summary, we believe that radar altimetry combined with high-resolution water level
334 modelling provides a viable alternative for validation of current geoid models, at least for
335 certain regions. Whether this holds for the future, with even lower geoid model errors,

336 depends on whether hydrodynamic modelling will be able to keep improving. Moreover,
337 with new altimetry technology we believe the observational gap between sea and land
338 may be closed: E.g. Fenoglio-Marc et al. (2015) find Cryosat-2 SSH fits to tide gauges in
339 the German Bight down to minimum RMS of 6cm (PRLM mode) and 7cm (SAR mode).
340 This would, together with satellite-only geoid models and airborne gravimetry provide a
341 basis for the validation of hydrodynamic modelling in the important coastal zone. Further
342 improvement in the coastal zone may be associated with altimetry retracking (e.g. Pas-
343 saro et al., 2015): on the one hand retracking may enable connecting altimetry and tide
344 gauges, on the other hand retracked footprints would contribute new and independent
345 information for validating geoid models.

6. References

- 346 Andersen, O. (1999): Shallow water tidal determination from altimetry: the *M4* con-
347 stituent, *Boll. Geod. Teor. Appl.* 40:427-437
- 348 Banner, K., K. Collins, and K. Massie (1979): *The North-West European Shelf Seas*,
349 Elsevier, Amsterdam, Noord-Holland
- 350 BKG (Bundesamt für Kartographie und Geodäsie) (2011): *Quasigeoid der Bun-*
351 *desrepublik Deutschland, Die Höhenreferenzfläche der Arbeitsgemeinschaft der Vermes-*
352 *sungsverwaltungen der Länder, GCG2011, www.geodatenzentrum.de/docpdf/quasigeoid.pdf*
- 353 Brockmann, J.M., N. Zehentner, E. Höck, R. Pail, I. Loth, and W.-D. Schuh (2014):
354 *EGM_TIM_RL05: An independent geoid with centimeter accuracy purely based on the*
355 *GOCE mission. Geophysical Research Letters*, 41(22):8089-8099

356 Bruinsma, S., Ch. Förste, O. Abrikosov, J. Marty, M.-H. Rio, S. Mulet, and S. Bon-
357 valot (2013): The new ESA satellite-only gravity field model via the direct approach.
358 *Geophysical Research Letters*, 40:3607-3612

359 Denker, H., J.-P. Barriot, R. Barzaghi, D. Fairhead, R. Forsberg, J. Ihde, A. Kenyeres,
360 U. Marti, M. Serrailh, and I. Tziavos (2009): The Development of the European Gravi-
361 metric Geoid Model EGG07. In: *Observing Our Changing Earth*, M. Sideris (Ed.). Proc.
362 IAG Symp. 133

363 Denker, H. (2013): Regional gravity field modelling: Theory and practical results. In:
364 *Science of Geodesy - II*, G. Xu (Ed.). Springer. 185-291

365 Dick, S., E. Kleine, S. Müller-Navarra, H. Klein, and H. Komo (2001): The operational
366 circulation model of BSH (BSCcmod), *Berichte des Bundesamtes für Seeschifffahrt und*
367 *Hydrographie*, No. 29/2001

368 Fenoglio-Marc, L., Dinardo, S., Scharroo, R., Roland, A., Dutour Sikiric, M., Lucas,
369 B., Becker, M., Benveniste, J., and R. Weiss (2015): The German Bight: A validation of
370 Cryosat-2 altimeter data in SAR mode, *Advances in Space Research* 55:2641-2656

371 Förste, Ch., S. Bruinsma, O. Abrikosov, J.-M. Lemoine, T. Schaller, H.-J. Götze, J.
372 Ebbing, J. Marty, F. Flechtner, G. Balmino, and R. Biancale (2014): EIGEN-6C4 The
373 latest combined global gravity field model including GOCE data up to degree and order
374 2190 of GFZ Potsdam and GRGS Toulouse. 5th GOCE User Workshop, Paris

375 Gatti, A., M. Reguzzoni, F. Migliaccio, and F. Sanso (2014): Space-wise grids of gravity
376 gradients from GOCE data at nominal satellite altitude. 5th GOCE User Workshop, Paris

377 Gruber, T. and HPF team (2015): GOCE gravity field models - overview and perfor-
378 mance analysis, presentation held at EGU General Assembly, 2015, Vienna

379 Hashemi Farahani, H., P. Ditmar, R. Klees, and X. Liu (2013) The static gravity field
380 model DGM-1S from GRACE and GOCE data: computation, validation and an analysis
381 of GOCE mission's added value. *Journal of Geodesy*, 87:843-867

382 Jensen, J. and C. Mudersbach (2006): Recent sea level variation at the North Sea and
383 Baltic Sea coastlines. *Proceedings of International Conference on Coastal Engineering*
384 (ICCE), Vol. 2, pp. 1764-1774, San Diego, USA

385 Huess, V (2001): Sea level variations in the North Sea from tide gauges, altimetry and
386 modelling, Scientific Report 01-08, Danish Meteorological Institute

387 Madsen, K., L. Høyer, and C. Tscherning (2007): Near-coastal satellite altimetry:
388 Sea surface height variability in the North Sea - Baltic Sea area, *Geophys. Res. Lett.*,
389 34:L14601

390 Mayer-Gürr, T., E. Kurtenbach, and A. Eicker (2010): ITG-Grace2010 gravity field
391 model. <http://www.igg.uni-bonn.de/apmg/index.php?id=itg-grace2010>

392 Mayer-Gürr, T., N. Zehentner, B. Klinger, and A. Kvas (2014): ITSG-Grace2014: a
393 new GRACE gravity field release computed in Graz. GRACE Science Team Meeting
394 (GSTM), Potsdam

395 Mayer-Gürr, T., R. Pail, T. Gruber, T. Fecher, M. Rexer, W.-D. Schuh, J. Kusche, J.-M.
396 Brockmann, D. Rieser, N. Zehentner, A. Kvas, B. Klinger, O. Baur, E. Höck, S. Krauss,
397 A. Jäggi (2015): The combined satellite gravity field model GOCO05s. EGU2015, Vienna

398 Naeije, M., R. Scharroo, E. Doornbos, and E.J.O. Schrama (2008): Global Altimetry
399 Sea Level Service: GLASS. final report NIVR/DEOS, NUSP-2 no. GO52320DEO

400 Passaro, M., P. Cipollini, and J. Benveniste (2015): Annual sea level variability of
401 the coastal ocean: The Baltic Sea – North Sea transition zone, Journal of Geophysical
402 Research (Oceans), 120(4):3061-3078

403 Pavlis, N., S. Holmes, S. Kenyon, and J. Factor (2012): The development and evalua-
404 tion of the Earth Gravitational Model 2008 (EGM2008). Journal of Geophysical Research,
405 117

406 Ray, R.D. (1999): A global ocean tide model from Topex/Poseidon altimetry:
407 GOT99.2, NASA Tech. Memo. 209478, 58pp., GSFC, Greenbelt, Maryland

408 Schall, J., A. Eicker, and J. Kusche (2014): The ITG-Goce02 gravity field model from
409 GOCE orbit and gradiometer data based on the short arc approach. Journal of Geodesy,
410 88:403-409

411 Slobbe, C., R. Klees, and B.C. Gunter (2014): Realization of a consistent set of vertical
412 reference surfaces in coastal areas. Journal of Geodesy, 88:601-615

413 Šprlak, M., C. Gerlach, and B. Pettersen (2015): Validation of GOCE global gravita-
414 tional field models in Norway, Newton's Bulletin 5:13-24

415 Voigt, C. and H. Denker (2015): Validation of GOCE gravity field models in Germany,
416 Newton's Bulletin 5:37-48

417 Weiss, R. (2013): Erfassung und Beschreibung des Meeresspiegels und seiner
418 Veränderungen im Bereich der Deutschen Bucht. PhD dissertation, TU Darmstadt,
419 <http://tuprints.ulb.tu-darmstadt.de/id/eprint/3661>

420 **Acknowledgments.**

421 We acknowledge Frank Jansen (BSH) for providing us with BSHmod model output,
422 Cornelius Slobbe (TU Delft) for providing NLGEO2013, and Robert Weiss (BfG) for
423 contributions during an early stage of the research.

Table 1. Geoid models used in this study (S = satellite-only, C = combined, RC = regional combined, SLR = satellite laser ranging data, SURF = surface data, ALTI = altimetry data, KIN = kinematic GNSS orbit data)

Type	Model	Reference	Data	Max. Res.
S	ITG-GRACE2010S	Mayer-Gürr et al. (2010)	7 yr GRACE	$n = 180$
	ITSG-GRACE2014S	Mayer-Gürr et al. (2014)	11 yr GRACE	$n = 200$
	ITG-GOCE02	Schall et al. (2014)	8 m GOCE	$n = 240$
	DIR_R5	Bruinsma et al. (2013)	4 yr GOCE + GRACE + LAGEOS	$n = 300$
	SPW_R4	Gatti et al. (2014)	3 yr GOCE	$n = 280$
	TIM_R5	Brockmann et al. (2014)	4 yr GOCE	$n = 280$
	DGM_1S	Hashemi Farahani et al. (2013)	7 yr GRACE + 14 m GOCE	$n = 250$
	GOC005S	Mayer-Gürr et al. (2015)	11 yr GRACE+ 4 yr GOCE + SLR + KIN	$n = 280$
C	EGM2008	Pavlis et al. (2012)	GRACE + SURF + ALTI	$n = 2190$
	EIGEN-6C4	Förste et al. (2014)	GRACE + GOCE + LAGEOS + SURF + ALTI	$n = 2190$
RC	EGG2008	Denker et al. (2009, updated) Denker (2013)	CHAMP + GRACE + SURF + ALTI	$1' \times 1'$
	NLGE02013	Slobbe et al. (2014)	DGM1-S + SURF + ALTI	$1 \text{ km} \times 1 \text{ km}$
	GCG2011	BKG (2011)	EIGEN-5C + EGM2008 + SURF + ALTI	$1.5' \times 1'$

D R A F T
February 4, 2016, 1:02pm

February 4, 2016, 1:02pm

D R A F T
1.5' × 1'

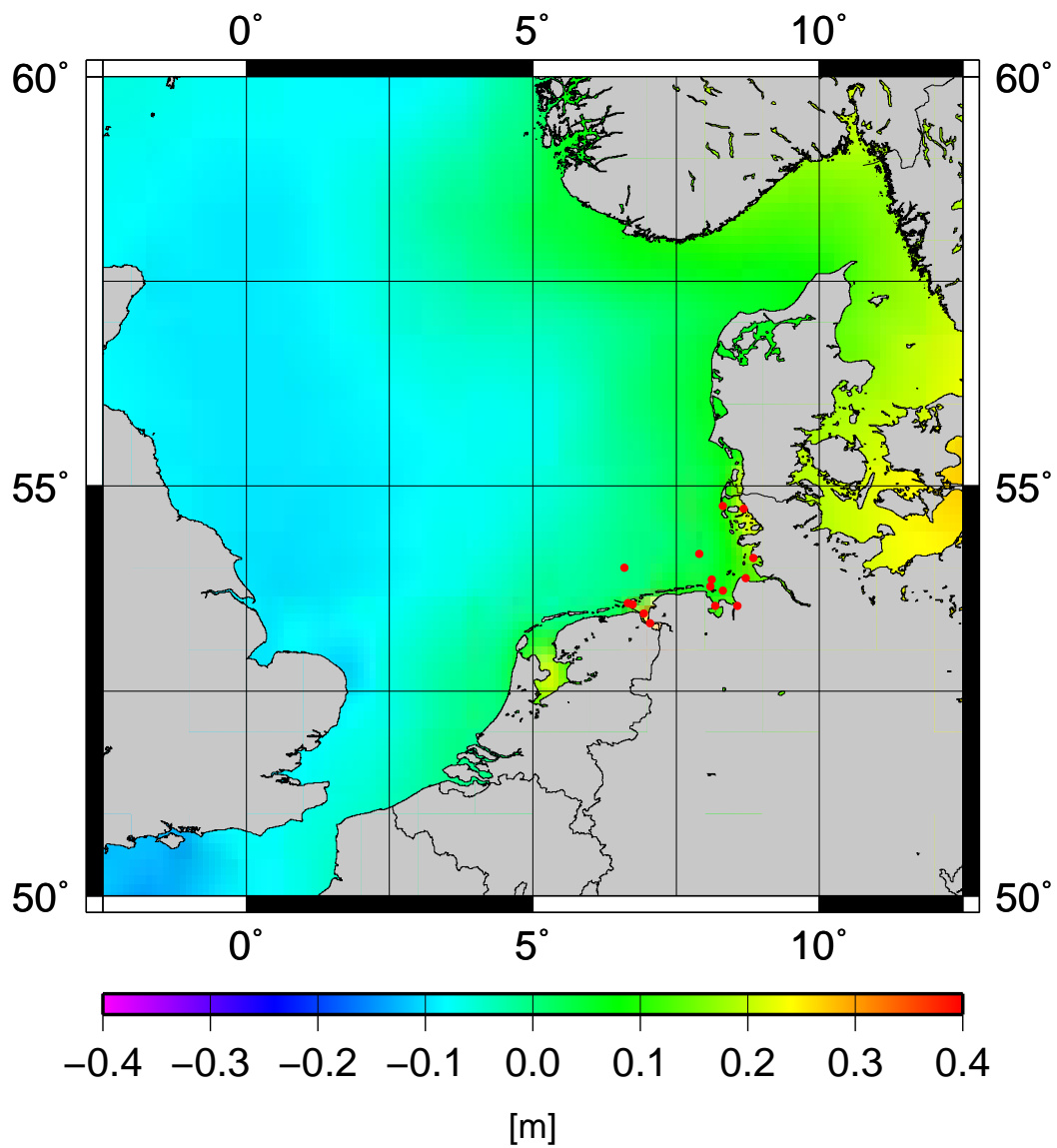


Figure 1. MDT from BSHmod version 3, 2000.0-2008.0

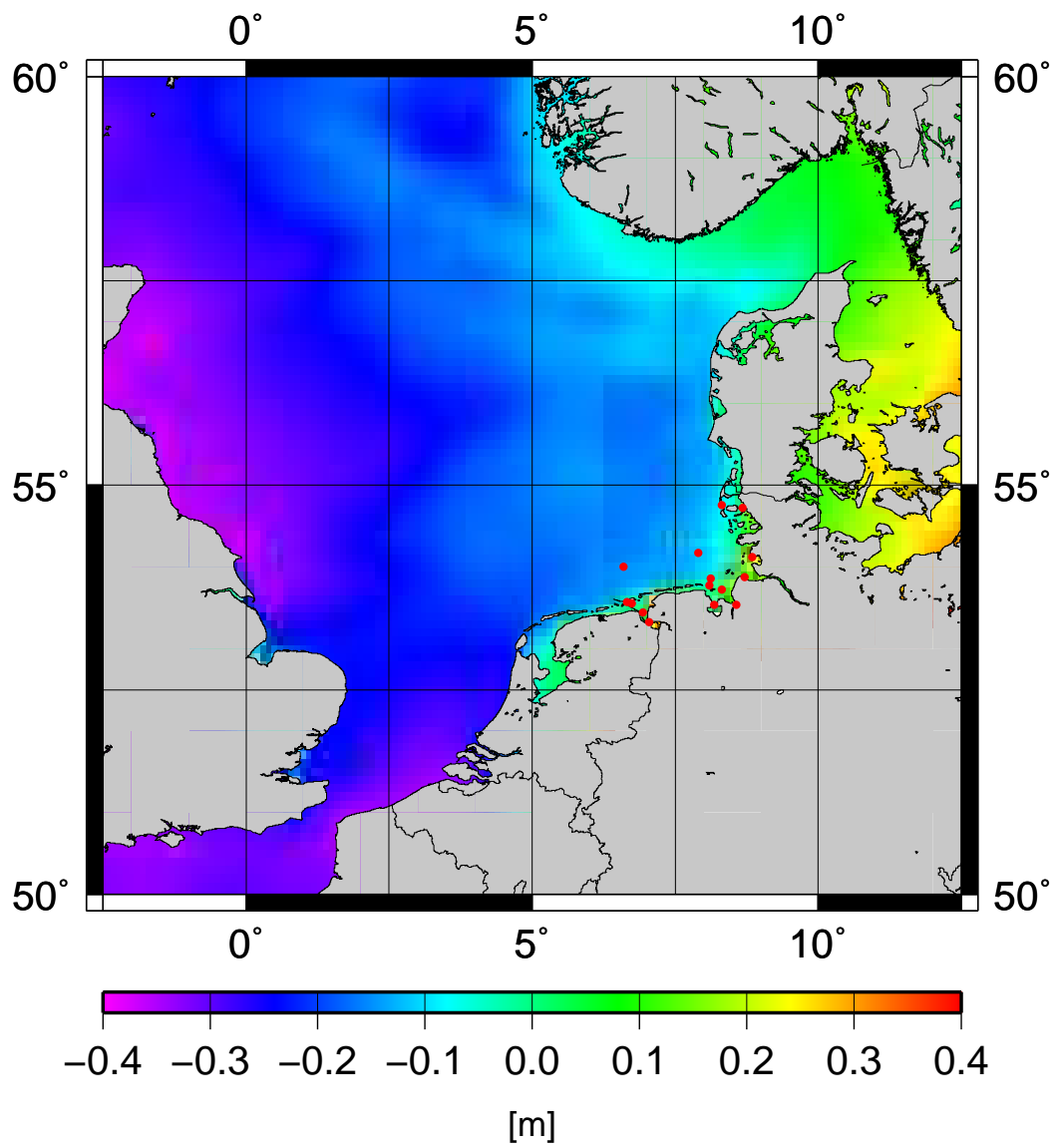


Figure 2. MDT from BSHemod version 4, 2008.0-2012.0

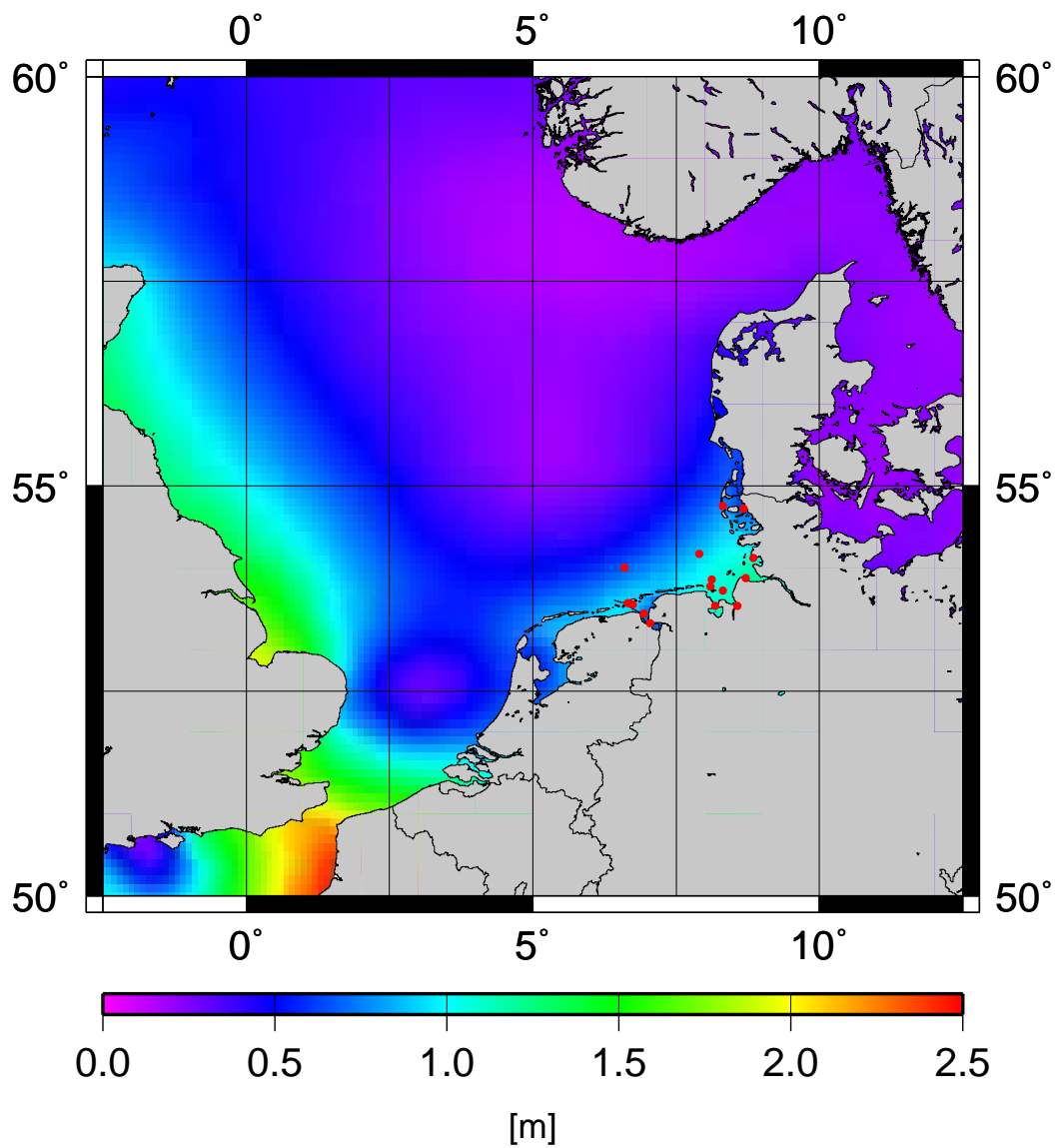


Figure 3. RMS water level variability from BSHcmod version 3, 2008.0-2012.0

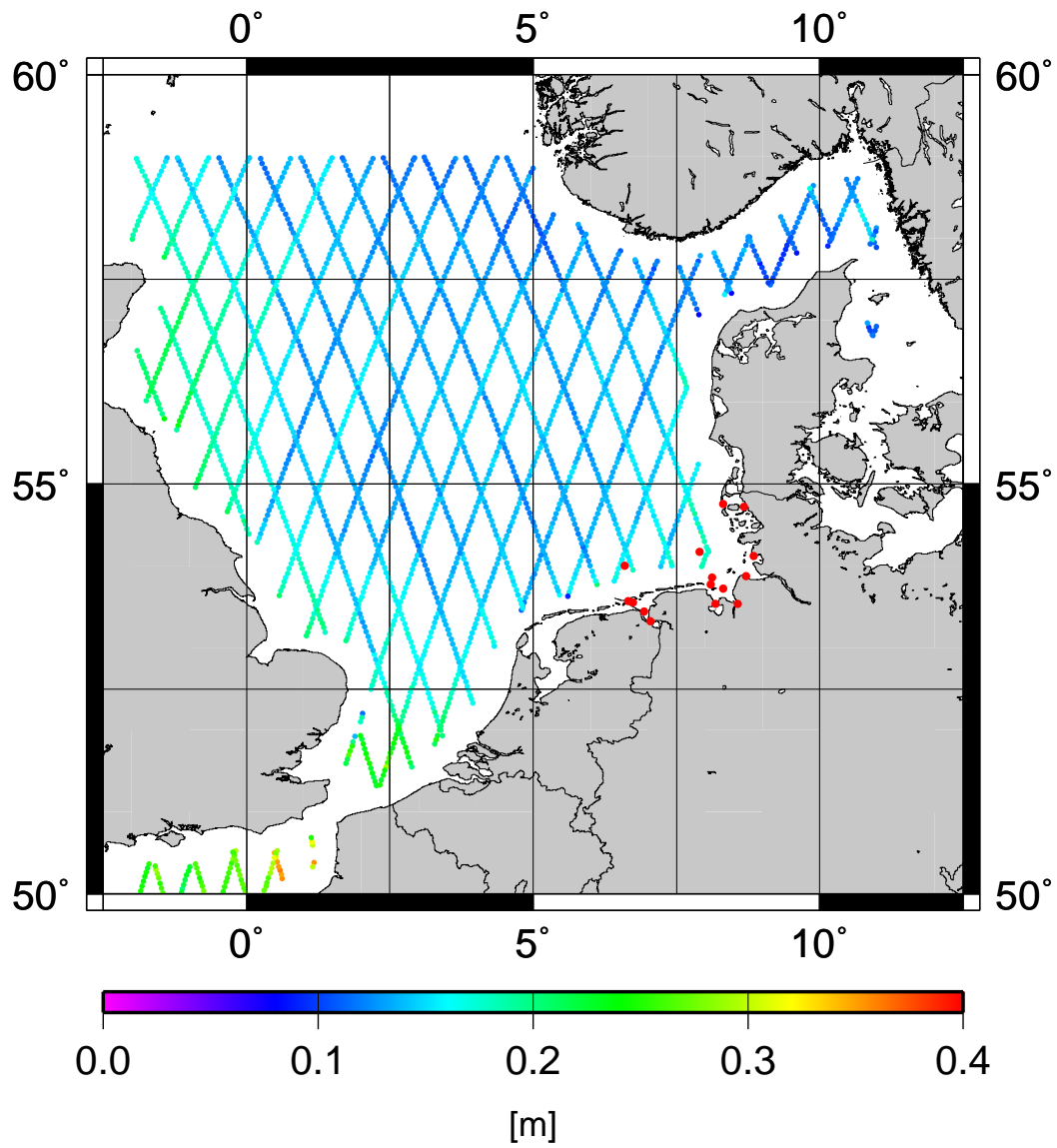


Figure 4. Standard deviation $\sigma_{N_i^{(a)}}$ of the altimetric-hydrodynamic water levels, obtained from averaging individual tracks

Table 2. RMS fit [m] of modelled water levels compared to tide gauge observations

TG	BSHcmod [m]	
	V.3 (2000.0-2008.0)	V.4 (2008.0-2010.0)
HOE2	0.22	0.17
TGDA	0.35	0.29
HELG	0.21	0.14
TGBU	0.35	0.23
FINO1	-	0.19
TGCU	0.26	0.18
LHAW	0.21	0.16
TGME	0.23	0.17
FLDW	0.33	0.27
BORS	0.21	0.14
TGBF	0.22	0.16
TGWH	0.44	0.27
TGBH	0.72	0.46
TGDU	0.28	0.17
TGKN	0.47	0.28

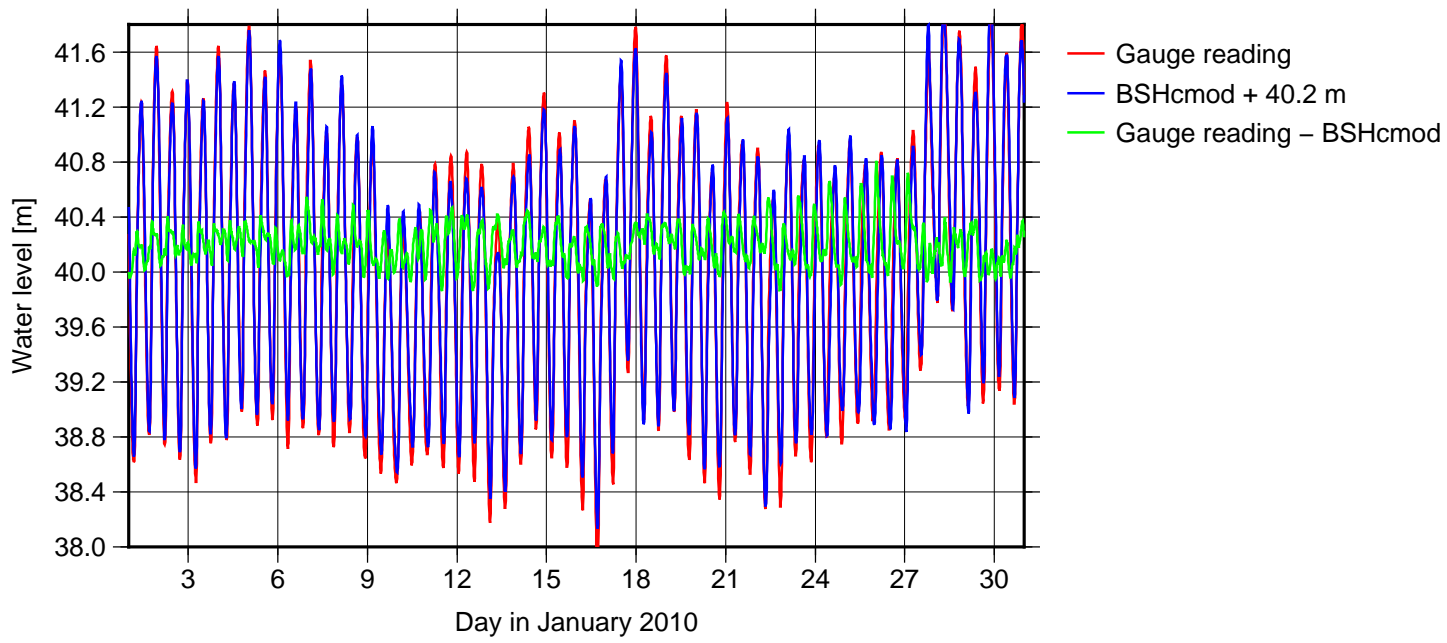


Figure 5. Modelled and observed water levels at TGBF

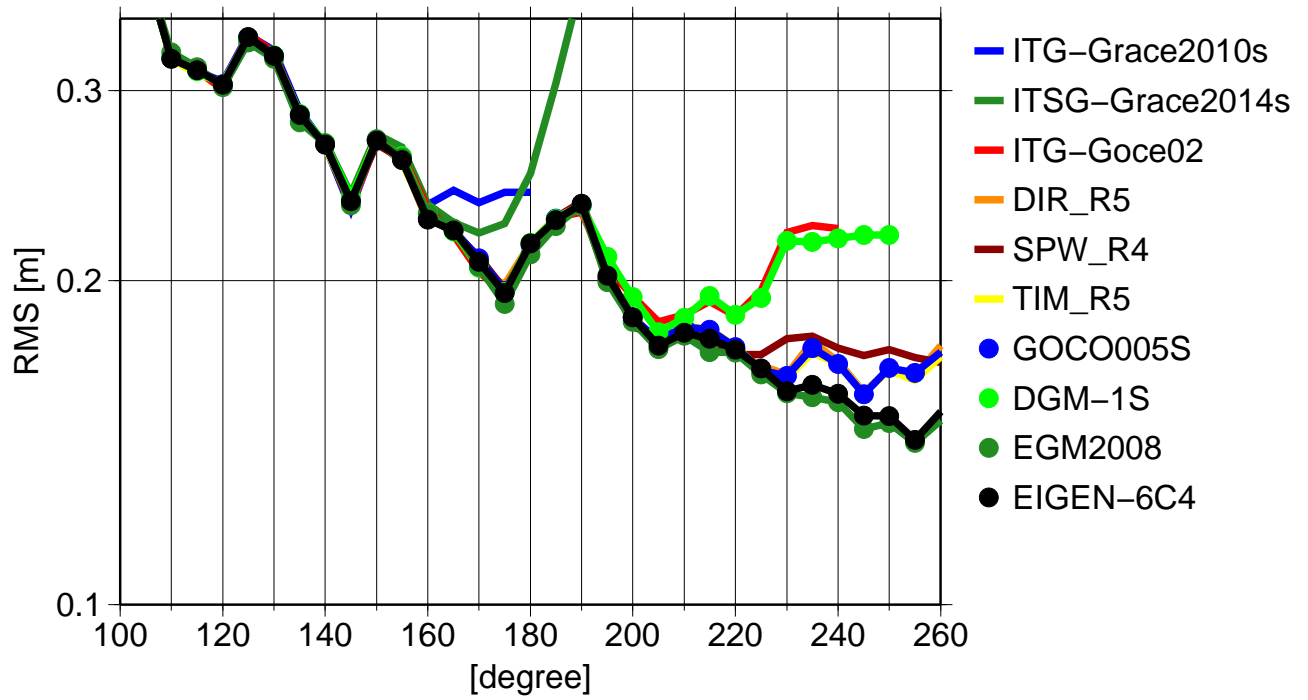


Figure 6. RMS misfit between gravimetric and altimetric-hydrodynamic geoid as a function of model truncation degree (without EGM2008 fill-up)

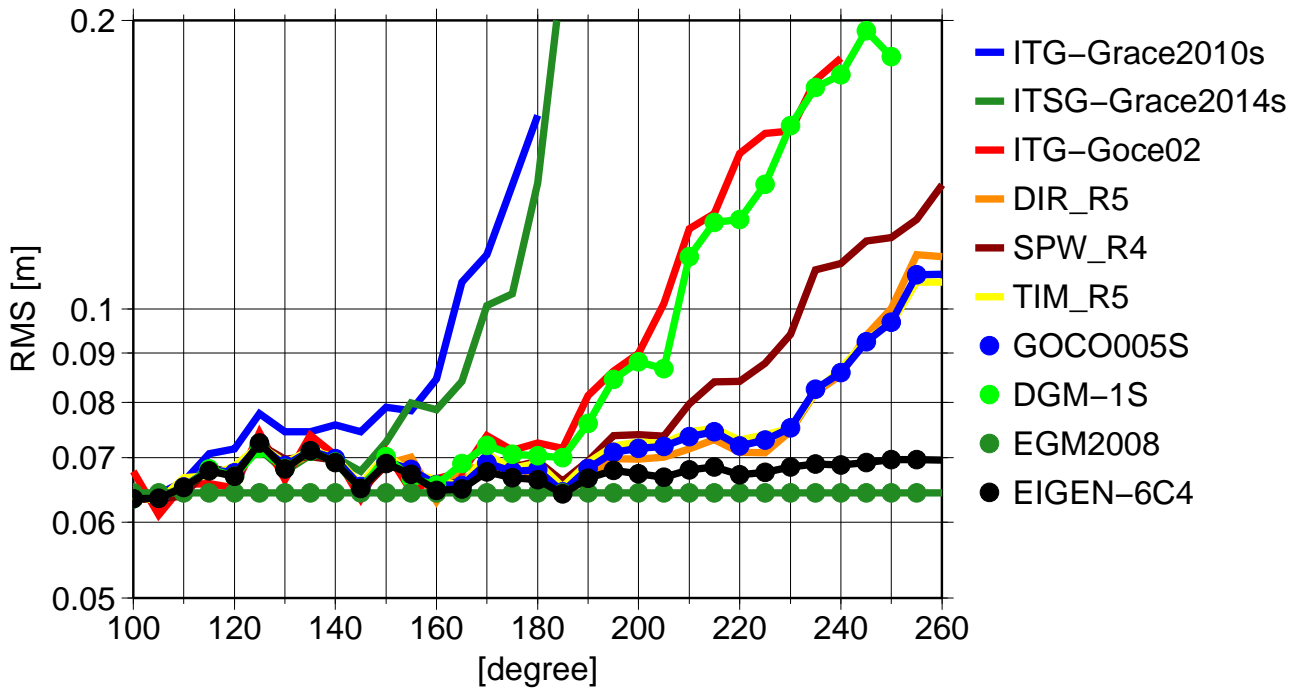


Figure 7. RMS misfit between gravimetric and altimetric-hydrodynamic geoid as a function of model truncation degree (with EGM2008 fill-up)

Table 3. RMS fit of regional geoid models

Model	RMS [m]	min [m]	max [m]
NLGE02013	0.067	-0.229	0.277
EGG08	0.064	-0.242	0.293
GCG2011	0.034	-0.117	0.093